



HAL
open science

ATES Contribution to the Housing Energy Balance: a Simple Assessment Methodology

Bernard Bourbiaux

► **To cite this version:**

Bernard Bourbiaux. ATES Contribution to the Housing Energy Balance: a Simple Assessment Methodology. Oil & Gas Science and Technology - Revue d'IFP Energies nouvelles, 2011, 66 (1), pp.21-36. 10.2516/ogst/2010015 . hal-01937339

HAL Id: hal-01937339

<https://ifp.hal.science/hal-01937339>

Submitted on 28 Nov 2018

HAL is a multi-disciplinary open access archive for the deposit and dissemination of scientific research documents, whether they are published or not. The documents may come from teaching and research institutions in France or abroad, or from public or private research centers.

L'archive ouverte pluridisciplinaire **HAL**, est destinée au dépôt et à la diffusion de documents scientifiques de niveau recherche, publiés ou non, émanant des établissements d'enseignement et de recherche français ou étrangers, des laboratoires publics ou privés.

ATES Contribution to the Housing Energy Balance: a Simple Assessment Methodology

B. Bourbiaux

IFP Energies nouvelles, 1-4 avenue de Bois-Préau, 92852 Reuil-Malmaison Cedex - France
e-mail: bernard.bourbiaux@ifpen.fr

Résumé — Contribution du stockage d'énergie thermique en aquifère au bilan énergétique lié à l'habitat : méthodologie d'évaluation rapide — La réduction des Gaz à Effet de Serre (GES) passe par un ensemble de solutions qui doivent être adaptées au contexte local des besoins et ressources en énergie, ainsi qu'aux variations de l'offre et la demande au cours du temps. Ce constat concerne en particulier la consommation d'énergie calorifique destinée à l'habitat. En effet, cette consommation de chaleur est saisonnière et rarement en phase avec la disponibilité des sources d'énergie alternatives ou renouvelables. Cet article étudie le stockage de chaleur dans des aquifères salins inexploités en tant que solution pour pallier ce déphasage entre production et consommation. Ce procédé concerne les réseaux de chaleur desservant un habitat concentré.

En premier lieu, une méthodologie quantitative est décrite pour dimensionner le projet de stockage d'énergie thermique en aquifère en fonction des caractéristiques de production et de consommation d'une part, et du coefficient de récupération de la chaleur stockée d'autre part. Le rôle important joué par ce facteur de récupération nous amène à une revue des pertes thermiques de diverses origines et à une étude de sensibilité à divers paramètres de réservoir, tels que son épaisseur, sa productivité et son hétérogénéité, dans l'optique de la sélection de l'aquifère et de la conduite du projet de stockage.

Abstract — ATES Contribution to the Housing Energy Balance: a Simple Assessment Methodology — *The reduction of Green-House Gas Emissions (GHGE) goes through a sum of solutions that need to be tuned to the local context in terms of energy needs and resources, and also to the demand and offer variations with time. The housing heat consumption is particularly concerned as it is seasonal and rarely in phase with the deliverability of alternative or renewable energy sources.*

This paper studies heat storage in saline untapped aquifers as a solution to overcome the time lag between production and consumption. This process applies to heat networks that supply dense housing complexes.

Firstly, a methodology is described to size an Aquifer Thermal Energy Storage (ATES) project as a function of the heat production and consumption characteristics on the one hand, and of the recovery factor of the stored heat on the other hand. The major role played by this recovery factor leads to a review of thermal losses of various origins and to a sensitivity study of influent reservoir parameters such as the aquifer thickness, productivity and heterogeneity, for the purpose of aquifer selection and storage project management.

INTRODUCTION – PROBLEM STATEMENT

In France, the residential and tertiary sector contributed in 2006 for 44% of the total energy used by all sectors and for 24% of total CO₂ emissions (2007 key data from the ADEME, the French Agency for the Environment and the Energy Management). In addition, the heat consumption is seasonal and rarely in phase with the deliverability of heat sources, in particular renewable ones. For instance, the fatal energy produced by industrial installations running from year's end to year's end does not find any use during summer, whereas heat consumption peaks often need resorting to fossil energy sources during winter. This problem is emphasized for a solar source, with a production completely out of phase with respect to needs. It may also constitute an opportunity to revitalize or extend geothermal projects.

This paper addresses the calorific needs of fairly-large cities equipped with heat networks. These heat networks can be fed by various energy sources, most often fossil or biomass combustibles, a geothermal resource if available, or heat from incineration plants. Waste heat from industries and fields of solar thermal panels may also be considered as other renewable heat sources. The power need for heat networks is commonly in the order of a few tens MW, corresponding to the housing needs of several thousands families. But this power need is subject to considerable changes over the seasons and may be four to five-fold higher during the winter period than during the summer period, depending on the latitude and climate.

Seasonal heat storage has long been tested and applied to satisfy winter calorific needs from summer excess heat. Aquifer Thermal Energy Storage (ATES), a process whereby aquifer water is used as the storage medium, has remained a prevailing storage technique since the seventies and eighties, although artificial reservoirs at surface (Schmidt *et al.*, 2003) and conduction-based Borehole Heat Exchangers (Busso *et al.*, 2003) were also developed later on. Reported ATES projects are quite numerous (Dickinson *et al.*, 2009; Lau *et al.*, 1986; Miller, 1986; Molz and Warman, 1978; Saugy, 1990; among many others) but generally concern aquifers that rarely exceed one or a few hundred meters in depth. Some of them combine the storage of warm water and chilled water for both heating and cooling purposes (Dickinson *et al.*, 2009). Only a few of them will be discussed later on, in reference with the specific context addressed in this paper.

Actually, most reported applications concern rather small-scale projects whereas herein, we focus on heat storages that can deliver a high heat power, in the ten-MW range, over a cold season period. Aquifer Thermal Energy Storage in deep saline aquifers is considered for two reasons that are the volume of water to be stored, and because regulations regarding the exploitation of shallow fresh water aquifers for other uses than fresh water consumption tend to become very restrictive. The counterpart however is a much higher capital expenditure linked to deeper wells, and the obvious necessity

to re-inject the produced brine. That is, a *doublet technique* has to be implemented as for most geothermal applications. The implementation is however made more complicated in the case of an ATES application than in the case of conventional geothermics, because the two wells have to inject or produce depending on the considered season. The aquifer management procedure illustrated in Figure 1 (Ungerer and Le Bel, 2006) is as follows. During the mild season, the reservoir brine is pumped at a given reservoir location and heated by the source via an exchanger, then re-injected into the same reservoir but at another distant location in order to constitute a “hot” bubble. That fluid circulation between the two wells is reversed during the cold season. The hot water is then produced in order to deliver its calorific energy to the heat network via an exchanger, and the cooled water resulting from that exchange is re-injected via the other well, thus constituting a “cold” bubble in the reservoir. The two previous steps constitute the basic annual storage cycle.

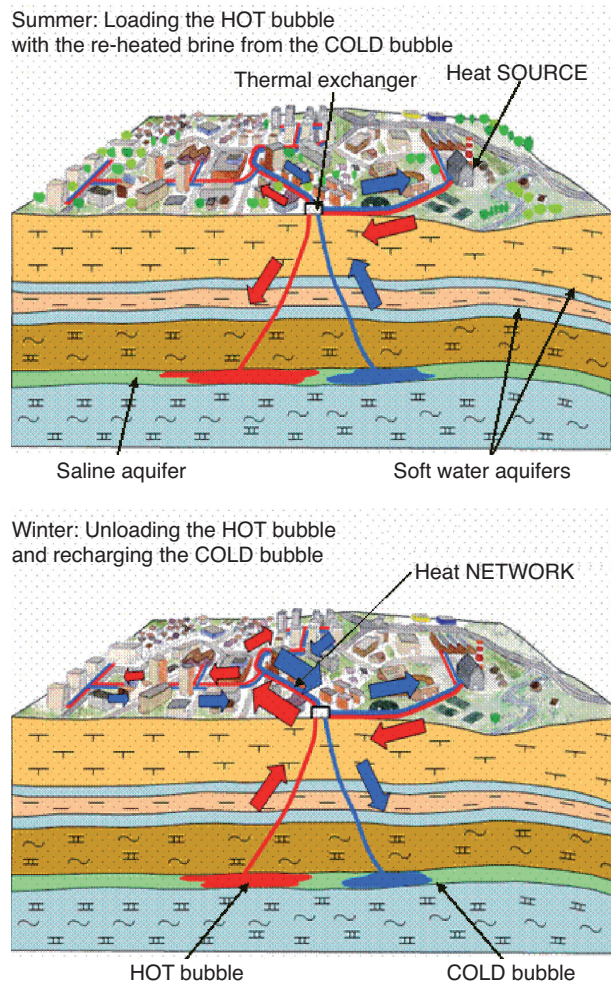


Figure 1

From Ungerer and Le Bel, *Revue des Ingénieurs des Mines* 423, Nov.-Déc. 2006. Illustration of the doublet technique: the annual heat storage cycle is shown in permanent regime, *i.e.* once thermal bubbles have been constituted.

Some aspects of ATEs history need to be recalled for our application purpose. Indeed, although heat storage in aquifers has very early been considered as a valuable solution for saving energy (Kazmann, 1978; Molz and Raymond, 1984), the ATEs concept did not really break through as an energy storage solution, partly because of the unfavourable conditions for energy saving solutions that prevailed during the post-crisis period of the eighties-nineties, and partly also because of the failure of a few pilot operations carried out under inadequate (Cormary *et al.*, 1978) or too-severe (Housse and Despois, 1985) conditions. The pilot experiment reported by Cormary *et al.* (1978) concerned a near-surface aquifer, only 3 to 10 m deep, from which only 30% of the stored heat was recovered because of the absence of confinement and hydraulic gradients leading to high losses. The project reported by Housse and Despois (1985) failed because it involved the storage of a high-temperature fluid, at 180°C, which led to troublesome deposits (salt precipitation) and to technological failures of well equipment.

Despite these failures, heat storage seems to have regained some interest in the recent years for obvious incentives of energy saving and management in conjunction with environmental concerns. Germany implemented various heat storage solutions (Schmidt *et al.*, 2003), including both artificial storage and geological storage. Regarding the aquifer storage solution, two ATEs projects (Kabus *et al.*, 2005; Sanner *et al.*, 2005) require particular mention as they tend to provide a renewed confidence in that technique.

The first one (Kabus *et al.*, 2005) is actually the sole reported ATEs project involving a fairly-deep aquifer, *i.e.* at a depth of 1200-1300 m. The project consists in storing the excess heat produced by a gas and steam cogeneration plant in summer in a low-temperature (53-55°C) geothermal aquifer that is feeding a district heat network having a load of 12 MW. Incentives for such a project were the excess of heat produced from the plant during summer, as well as the low temperature of the geothermal water that required the installation of heat pumps. Two doublets were implemented. A sophisticated well equipment, with fiber-glass riser and casing, was designed to face aggressive fluid conditions. Alternated injection and production were ensured through the use of a submersible pump, water being produced via the pump riser and injected through the annular space. A heat recovery of 88 000 MWh out the 120 000 stored MWh is reported, *i.e.* a recovery efficiency of 73%.

The second project (Sanner *et al.*, 2005) is still more sophisticated as it involves Underground Thermal Energy Storage into two distinct aquifers at fairly-low depths, 60 and 320 m. The shallower one stores cold water during winter for cooling purposes in the following summer. The deeper one stores waste heat from an electric power generation plant during summer for heating purposes during winter. Absorption heat pumps are also components of the whole system to supplement cooling or heating requirements if necessary.

Simulated retrieved-to-stored recovery ratios equal 93% and 77% respectively for the cold aquifer and for the warm one.

These two recent projects look attractive in terms of energy recovery efficiency and justify reconsidering the feasibility of the ATEs concept with the help of recent technological advances. Energy supply and environmental concerns are obviously the other incentives for the present study.

The paper is organized as follows. First, a methodological approach is presented for sizing an ATEs project with respect to the characteristics of energy consumption and heat sources. Then, the recovery performance of the aquifer storage is analyzed as a function of determinant reservoir static and dynamic properties. Two types of heat sources are considered, a constant-flux waste heat source and a solar energy source out of phase with the heat consumption.

The methodology starts with a quantification of seasonal storage requirement on the basis of a preliminary characterization of heat consumption and production profiles.

1 SEASONAL HEAT STORAGE REQUIREMENT

The assessment of heat storage needs goes through the confrontation of heat consumption and production profiles over a year cycle.

1.1 Characterization of Heat Consumption

We consider typical housing calorific energy needs as shown by the consumption profile of Figure 2, drawn from the methodological monitoring guide of combined solar systems (Letz, 2004) found on INES website <http://www.ines-solaire.com/>. The heat network demand for a few thousands of dwellings of a urban area would obviously follow the same trend.

The seasonal variations in energy needs can be characterized by a criterion, named the heat *Consumption Seasonality Factor*, denoted *CSF*, and defined as follows.

Considering the year-averaged power consumption equal to \bar{C} , the durations of the “winter” and “summer” periods, respectively Δt_w and Δt_s , are firstly defined as the time durations over which the power need is higher (resp. lower) than \bar{C} , that is:

- $C(t) > \bar{C}$ over the “winter” period of time Δt_w , with C_w the average power need over that period,
- $C(t) < \bar{C}$ over the “summer” period of time Δt_s , with C_s the average power need over that period.

From the above definitions, it follows that:

$$\int_{\Delta t_w} (C(t) - \bar{C}) dt = \int_{\Delta t_s} (\bar{C} - C(t)) dt$$

or, using season-averaged values of consumption:

$$(C_w - \bar{C}) \Delta t_w = (\bar{C} - C_s) \Delta t_s$$

The *Consumption Seasonality Factor* is then defined with respect to the yearly-averaged power need as the ratio between the additional energy required during the “winter” period and the total yearly consumption, or reversely as the ratio between the excess energy available for other purposes during the “summer” period and the total yearly consumption, that is:

$$CSF = \frac{\int_{\Delta t_w} (C(t) - \bar{C}) dt}{\int_{\text{year}} C(t) dt} = \frac{\int_{\Delta t_s} (\bar{C} - C(t)) dt}{\int_{\text{year}} C(t) dt}$$

or

$$CSF = \frac{(C_w - \bar{C})\Delta t_w}{C(\Delta t_w + \Delta t_s)} = \frac{(\bar{C} - C_s)\Delta t_s}{C(\Delta t_w + \Delta t_s)} \quad (1)$$

For the consumption profile shown in Figure 2, the “winter” and “summer” periods are both equal to 6 months, and \bar{C} , C_w and C_s are respectively equal to 2.3, 3.6 and 1.0 kW.

CSF then equals 28%, meaning that 28% of the total consumed energy should be stored in “summer” and entirely-recovered in “winter” if all that energy were supplied by a constant-flux energy source.

CSF is a useful criterion for characterizing the seasonality of energy needs independently of the energy source characteristics.

CSF is theoretically comprised between:

- 0 if the energy consumption is constant all during the year ($\bar{C} = C_w = C_s$), *i.e.* if there are no seasonal contrasts; and,
- 1 if all the energy is consumed during an “instantaneous” intense winter period ($C_s = 0$) and $\Delta t_w \ll \Delta t_s$.

Actually, a significant energy need, C_s , remains latent during summer, for sanitary hot water supply. CSF should hardly exceed 0.5, a value corresponding to equal “winter” and “summer” periods and no energy consumption in summer.

1.2 Characterization of Heat Production

Electricity and combustion of fossil sources, whether coal, oil or natural gas, still constitute energy supply solutions to meet temporary consumption peaks of the heat demand. They are not considered herein as the present trend is toward the use of alternative CO₂-free and/or energy-efficient sources.

Among such alternative sources, *waste heat sources*, including urban incineration plants and energy-intensive plants, are prone to a valorisation through medium-to-large heat networks because that heat is produced massively and locally. Most sectors of the raw materials industry are concerned, such as the iron and steel industry, cement, glass, paper and raw chemicals factories. The waste heat from these industrial sources is most always produced on a *constant-power basis* independently of the housing energy consumption market. That is, a complete valorisation of Waste Heat

calls for storage solutions if a heat market exists in the close neighbourhood of such sources. To that respect, the heat produced from *household waste combustion* has a specific advantage in the sense that the amount of available energy from waste combustion is in proportion to the city population and therefore also proportional to the heat requests for given housing conditions in terms of thermal insulation, waste production and recycling.

Renewable energy sources are also considered to satisfy the housing calorific energy needs. Both geothermal energy and solar energy are concerned. *Geothermal energy* is particularly well suited to meet seasonal housing demand because of its flexibility. On the contrary, *solar energy* plants probably constitute sources that are mostly out of phase with respect to heating needs. A typical solar thermal power production profile is shown in Figure 2 for a European location, Zürich, Switzerland (from INES website data base).

Similarly to the *Consumption Seasonality Factor* (CSF), one can define another indicator, denoted as the *Production Seasonality Factor*, PSF , and formulated as:

$$PSF = \frac{\int_{\Delta t_s} (P(t) - \bar{P}) dt}{\int_{\text{year}} P(t) dt} = \frac{\int_{\Delta t_w} (\bar{P} - P(t)) dt}{\int_{\text{year}} P(t) dt}$$

or

$$PSF = \frac{(P_s - \bar{P})\Delta t_s}{P(\Delta t_w + \Delta t_s)} = \frac{(\bar{P} - P_w)\Delta t_w}{P(\Delta t_w + \Delta t_s)} \quad (2)$$

with \bar{P} as the average yearly power delivered by the heat source, P_s (P_w) the average power delivered during the summer (winter) period defined similarly as above (*i.e.* the periods of time over which $P(t)$ is respectively higher (lower) than \bar{P}) and Δt_s (Δt_w) the duration of the summer (winter) period, assuming summer is the period of highest production as for a solar source. PSF characterizes the seasonality of the heat production and represents the fraction of the yearly-produced power to be stored in “summer” and entirely-recovered in “winter” in order to meet a constant power need, \bar{C} , equal to the year-averaged power production, \bar{P} .

For the solar production profile shown in Figure 2, corresponding to the irradiation observed in Zürich, the “winter” and “summer” periods are again close to 6 months. P_w and P_s are respectively equal to 1.5 and 3.1 kW if one refers to an average yearly power production that is exactly equal to the average heat need (2.3 kW) of a dwelling-house.

PSF is then equal to 18%, meaning that the energy to be stored in “summer” and entirely-recovered in “winter” to feed a constant-flux demand represents 18% of the total produced energy over a year.

Alike CSF , PSF characterizes the seasonality of energy production independently of the energy demand.

1.3 Theoretical Seasonal Heat Storage Requirement

The need for a seasonal heat storage depends on both the anti-coincidence in time between the heat demand and the energy availability, and the magnitude of consumption and/or production fluctuations.

Considering heat consumption and production profiles of Figure 2, the need for heat storage can be quantified as follows. First, these consumption and production profiles are scaled with respect to one another in order that the respective year-averaged values of consumed and produced powers are equal. Either the consumption profile or the production profile is scaled, whether respectively the heat source or the heat market is fixed. A scaling of the heat production profile was adopted in Figure 2, with the average monthly consumption of a house taken as the power reference.

The Difference, $PCD(t)$, between the Production profile $P(t)$ and the Consumption profile $C(t)$, quantifies the need for energy storage to satisfy exact equilibrium between consumption and production over a yearly cycle (Fig. 3). That representation directly shows the period of time over which the energy produced in excess of consumption should be stored and the complementary cold period over which that energy should be recovered to satisfy consumption, that is:

- storage when $PCD(t) > 0$,
 - recovery of the stored energy when $PCD(t) < 0$,
- with the amount of energy to be stored then recovered equal to:

$$\int_{t, PCD(t) > 0} PCD(t) dt = - \int_{t, PCD(t) < 0} PCD(t) dt$$

Energy production and consumption profiles (the production is scaled to the total annual consumption)

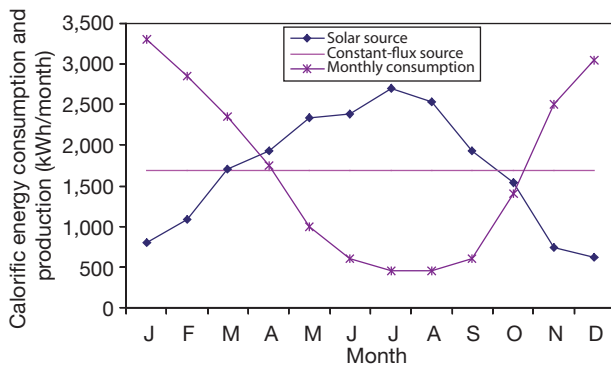


Figure 2

Heat consumption and production profiles. The monthly consumption profile represents the heating and hot sanitary water needs of a dwelling-house (100 m², 200 kWh/m²/year). Heat production is scaled with respect to the consumption profile for a constant- or a variable-flux source. Regarding the solar (variable-flux) source, the profile corresponds to the power production from thermal collectors located in Europe (Zürich).

Misfit profile between consumption and production (the production is scaled to the total annual consumption)

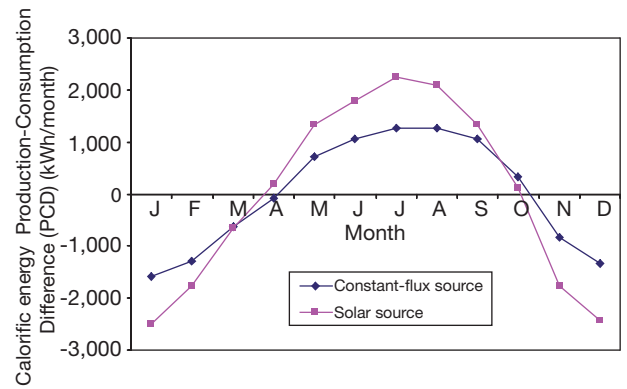


Figure 3

Production-Consumption Difference profile (PCD).

One must mention that, due to short-periodicity climate fluctuations, the uniqueness of the time values, for which the sign of PCD changes from positive to negative (and from negative to positive), is obtained for a sufficiently-coarse time discretization as for the monthly representation considered above, but not for a fine discretization, such as daily records for instance.

A heat STORage Requirement indicator, $STOR$, can then be defined as the ratio between the heat to be stored during the low-consumption season and the total yearly heat consumption, that is:

$$STOR = \frac{\int_{t, PCD(t) > 0} PCD(t) dt}{\int_{year} C(t) dt} \quad (3)$$

In the case of a constant-flux heat source, $STOR$ is obviously equal to the consumption seasonality factor, CSF .

In the case of a variable-flux heat source, typically a solar source, the value of the heat storage indicator depends on how far the consumption and the production are out of phase. For a solar source, production and consumption are most often nearly in anti-coincidence (Fig. 2), hence the storage requirement indicator is close to the sum of production and consumption seasonality factors, that is $STOR \approx PSF + CSF$. In the general case, one can write:

$$0 \leq STOR \leq PSF + CSF$$

- $STOR = 0$ for a source in coincidence with consumption,
- $STOR = CSF$ for a constant-flux source,
- $STOR = PSF + CSF$ for a variable-flux source in anti-coincidence with consumption.

CSF , PSF and $STOR$ values for the consumption-production profiles shown in Figure 2 are summarized in Table 1 below. As expected for a solar source, $STOR$ is very close to the sum of CSF and PSF , i.e. solar production and heat consumption are completely out of phase.

TABLE 1

Values of consumption, production and storage requirement indicators for constant-flux and solar sources examples

	CSF	PSF	CSF + PSF	STOR
Constant-flux source	28.2%	0%	28.2%	28.2%
Solar source	28.2%	17.9%	46.1%	44.8%

In practice, one has to account for heat losses during the whole storage-recovery cycle in order to assess the size of the source (possibly completed with a spare supply) satisfying consumption needs, or to limit the consumption market (number of dwellings) if a fixed-flux source is considered. That is, palliating the production-consumption misfit through a heat storage solution goes through the assessment of the heat store recovery efficiency, as discussed in the following section.

2 SIZING A HEAT STORAGE PROJECT – SENSITIVITY TO THE HEAT RECOVERY EFFICIENCY AND TO THE PRODUCTION/CONSUMPTION CHARACTERISTICS

For a theoretical 100%-efficient heat store, all the stored heat is recovered during the high-consumption period, that is, such a store satisfies the following energy balance equation:

$$\int_{t, PCD(t)>0} PCD(t)dt = - \int_{t, PCD(t)<0} PCD(t)dt \quad (4)$$

For an actual heat store, only a fraction, R , of the stored heat is recovered because of the heat losses occurring during the storage and recovery operations. We define the heat recovery efficiency, R , on a yearly-cycle basis, as the fraction of the stored heat amount that is recovered from the ATES and actually delivered to the heat network. R accounts for all heat losses, taking place essentially within the aquifer and during fluid transport to or from the aquifer store during loading and unloading steps.

In order to satisfy a given consumption need, the source has to be oversized to compensate for these losses. We then define α as the factor or ratio of source over-sizing with respect to the average consumption power in order to satisfy the following balance between the recovered heat from the ATES and the winter heat needs:

$$R \int_{t, \alpha P(t) > C(t)} (\alpha P(t) - C(t))dt = \int_{t, \alpha P(t) < C(t)} (C(t) - \alpha P(t))dt \quad (5)$$

Conversely, if the calorific production is fixed and cannot be adjusted to the demand, as is the case for most industrial waste heat sources, then a reduction factor ($1/\alpha$) is applied to the consumed power:

$$R \int_{t, P(t) > \frac{C(t)}{\alpha}} (P(t) - \frac{C(t)}{\alpha})dt = \int_{t, P(t) < \frac{C(t)}{\alpha}} (\frac{C(t)}{\alpha} - P(t))dt$$

The former situation involving a flexible production is assumed in the following.

For a given value of the recovery factor R , the oversizing factor α satisfies the following equation:

$$\alpha = \frac{\int_{t, \alpha P(t) < C(t)} C(t)dt + R \int_{t, \alpha P(t) > C(t)} C(t)dt}{\int_{t, \alpha P(t) < C(t)} P(t)dt + R \int_{t, \alpha P(t) > C(t)} P(t)dt} \quad (6)$$

An iterative solving procedure is required to determine α because the integration intervals are functions of that unknown.

For an approximate analysis of the recovery impact on α , we will assume fixed storage and recovery periods, denoted again as Δt_s and Δt_w for “summer” and “winter”.

Under such conditions of fixed storage and recovery periods, we can simply formulate the over-sizing factor as:

$$\alpha = \frac{C_w \Delta t_w + R C_s \Delta t_s}{P_w \Delta t_w + R P_s \Delta t_s} \quad (7)$$

with C_w , P_w and C_s , P_s being respectively the average consumed and produced powers during the “winter” (recovery) and “summer” (storage) periods. These power values are drawn from the actual consumption and production profiles scaled with respect to one another.

The evolution of α for various recovery factor values is given in Figure 4 for a constant-flux source and for the solar variable-flux source described before (Fig. 2), and loading/unloading periods of 6 months each.

Note that in practice, heat storage and recovery would actually be performed over the periods of time when consumption is significantly low or high, *i.e.* over nearly-invariable periods of time, generally not exceeding 4 or 5 months. For instance, the period of heat recovery from the store may be limited to the months over which the Consumption-Production Difference, CPD , is at least equal to half the maximum monthly CPD value, which leads to a “winter” period of 4 months from November to February in the example under consideration in this paper. Reversely, the period of heat storage may be limited to the period over which the Production-Consumption Difference, PCD , exceeds half of the maximum monthly PCD , which leads to a “summer” period of 5 months from May to September in the studied example. Above definition for α still stands provided that inactivity periods are excluded, however, a small energy amount is then either lost or missing during the intermediate periods separating the cold and hot seasons.

Figure 4 shows that for a seasonal storage recovery efficiency of 50%, the annual production from a constant-flux source must be nearly 20% more than the effective annual heat consumption in order to meet that heat consumption all through the year. Assuming the same recovery efficiency, a solar source must be oversized by 36% with respect to the heat consumption because of the higher contribution of the ATES to the heat supply in that case.

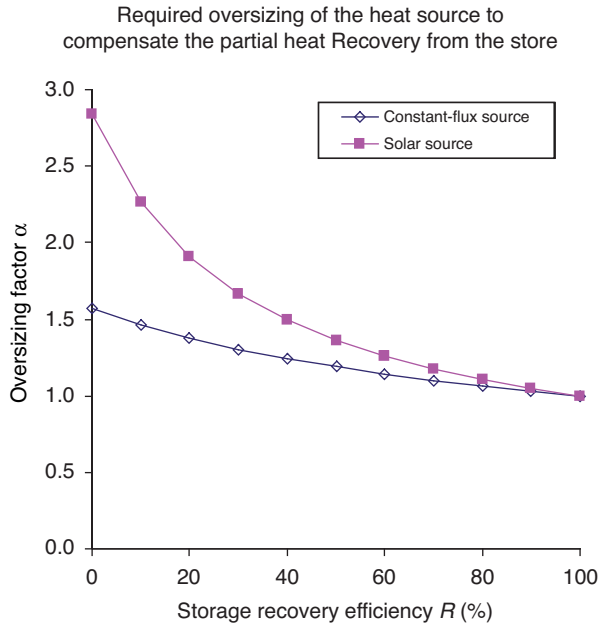


Figure 4

Required oversizing of the heat source to compensate the limited heat recovery from the store, for the heat production-consumption data shown in Figures 2 and 4 for a full-year heat store activity (storage and recovery periods of 6 months).

As expected, the heat source over-sizing factor, α , is all the larger as the recovery factor is low. Moreover, α does not vary linearly with R but increases all the faster as the recovery gets lower.

That observation clearly underlines the determinant role played by the recovery efficiency in a heat storage project. Moreover, the previous analysis assumes that other consumption constraints remain satisfied, in particular the minimum delivered temperature, which cannot be lower than a certain limit (around 60°C) for sanitary reasons. Such a constraint may actually not be satisfied for a low-efficiency ATEs and may then require either the use of an additional heat source to raise the fluid temperature at the heat network entry point, or a higher temperature of the stored fluid assuming that the heat source can deliver such a temperature.

For the purpose of pre-designing an ATEs project, a general relationship is proposed hereafter to determine α as a function of the consumption and production indicators and of the estimated value of the recovery efficiency.

General relationship between α and the production and consumption characteristics, and the storage recovery efficiency R .

If production and consumption are assumed in anti-coincidence (including the constant-flux source case), then the over-sizing factor, α that is the ratio \bar{P}/\bar{C} between the year-averaged power of the source and the year-averaged consumption power, can be expressed as a function of the

above-defined production and consumption indicators, PSF and CSF , the storage recovery efficiency, R , and the relative duration of the unloading period, $\beta = \Delta t_w / (\Delta t_w + \Delta t_s)$. For a full-year storage activity duration ($\Delta t_w + \Delta t_s = 12$ months), the following relationship can be established:

$$\alpha = 1 + (PSF + CSF) \frac{1 - R}{\beta + R(1 - \beta) - PSF(1 - R)} \quad (8)$$

This equation is derived from Equation (7) where the produced and consumed powers, P_w , P_s , and C_w , C_s are replaced by their respective expressions as a function of \bar{P} , PSF , β and \bar{C} , CSF , β . For given consumption and production characteristics, CSF and PSF , a given relative duration of the unloading period β , and a given heat recovery efficiency, R , one can then directly determine the average production power, $\alpha \bar{C}$, that is required to satisfy the average yearly consumption power, \bar{C} . Table 2 gives examples of the use of such a formula for equal durations (6 months) of the loading and unloading periods. The source oversizing factor, α , is determined as a function of CSF , of PSF taken equal to either 0 (constant-flux source) or CSF , and of the heat recovery efficiency. Figure 5 illustrates these results.

Considering a consumption profile characterized by a seasonality factor, CSF , equal to 0.3, Table 2 indicates that the power of a constant-flux source should be 20% larger than the yearly average consumption power ($\alpha = 1.2$), if heat is stored during “summer” and recovered during the cold season with a recovery efficiency equal to 50%. But in the case of a solar source characterized by the same seasonality factor of 0.3, the yearly-produced heat amount has to be 50% larger than the consumed heat amount ($\alpha = 1.5$) to meet that demand all through the year.

Figure 5 illustrates again the impact of the heat recovery efficiency, with a non-linearity that is emphasized when a high contribution of the heat storage to the overall energy supply is required, that is for a high seasonality of the demand and/or the energy source. These charts are only aimed at providing an order of magnitude of required power values when pre-designing an ATEs project.

We will now focus on the factors influencing the performance of a heat storage.

In order to assess the technical and economical feasibility of an ATEs, the different reasons for heat losses are reviewed and discussed hereafter, using consumption-production characteristics detailed before.

3 FACTORS INFLUENCING THE RECOVERY EFFICIENCY OF AN AQUIFER HEAT STORE

The recovery from the heat store depends on the size and surface/volume ratio of the thermal bubble set in place in the aquifer. The surface/volume ratio is determined by the aquifer thickness and porosity for a given stored volume, and

conversely. For that reason, before discussing the effect of heat transfer mechanisms and parameters, we need to specify the order of magnitude of heat store size.

3.1 Typical Aquifer Store Size for Urban Heat Networks

In fairly-large cities, typical heat network powers lie in the 10–100 MW range. We will consider for instance a heat market of 10 000 families living in conventional housings. The annual heat consumption per housing (100 m² each) is the one illustrated in Figure 2, that is 20 300 kWh, corresponding to 203 kWh/(m².year), including heating and sanitary hot water supply. That figure is in line with the energy consumption of a housing park built several decades ago and characterized by a poor energetic efficiency. Then the total calorific need to be supplied by the heat network is 203 000 MWh per year, which corresponds to an average calorific power equal to 23.2 MW. For a constant-flux source exactly sized on an annual basis to the consumption profile of Figure 2, one can determine that an energy amount of 57 300 MWh is produced in excess to the consumption needs during 6 months (May to October). That energy has to be stored during these months with store loading powers ranging from 4.4 to 17.1 MW (on a month-average basis) and recovered from November to April with store unloading powers ranging from 1.1 MW to 21.2 MW. Considering a 50% recovery efficiency, Figure 4 indicates that a constant-source power needs to be oversized

by about 20% to compensate for the corresponding thermal losses. Keeping the same consumption profile, this leads to the storage of 77 800 MWh from May to October, with a maximum loading power of 21.8 MW. Finally, assuming the effective temperature drop on the heat network exchangers equals 30°C, one infers that the stored aquifer brine volume is close to 2.2 million m³ and the maximum transfer rate from the store to the surface is 630 m³/h.

In summary, taking into account reasonable values of the temperature drop and store over-sizing (*i.e.* 30°C and 20%), one can keep in mind the following orders of magnitude for stored water volume and nominal (maximum) volumetric transfer rate per 10-MW of heat power:

- a stored brine volume, V_{inj} , in the order of 1 million cubic meters,
- a nominal volumetric transfer rate of around 300 cubic meters per hour.

The following discussions regarding heat losses and thermal efficiency of the store are based on such orders of magnitude.

For a total net thickness of porous and permeable layers equal to H and an average porosity equal to ϕ , one can estimate the hydraulic radius of the stored water cylindrical bubble as:

$$R_h = \sqrt{\frac{V_{inj}}{\phi \cdot \pi H}} \quad (9)$$

TABLE 2

Values of the source over-sizing factor, α , as a function of the consumption seasonality factor, of the production seasonality factor (assumed either nil or equal to CSF) and the heat storage recovery efficiency (with $\beta = 0.5$)

Constant source power	R	CSF ($PSF = 0$)	0.05	0.1	0.15	0.2	0.25	0.3	0.35	0.4	0.45	0.5
		0.1	1.082	1.164	1.245	1.327	1.409	1.491	1.573	1.655	1.736	1.818
0.2	1.067	1.133	1.200	1.267	1.333	1.400	1.467	1.533	1.600	1.667		
0.25	1.060	1.120	1.180	1.240	1.300	1.360	1.420	1.480	1.540	1.600		
0.3	1.054	1.108	1.162	1.215	1.269	1.323	1.377	1.431	1.485	1.538		
0.4	1.043	1.086	1.129	1.171	1.214	1.257	1.300	1.343	1.386	1.429		
0.5	1.033	1.067	1.100	1.133	1.167	1.200	1.233	1.267	1.300	1.333		
0.6	1.025	1.050	1.075	1.100	1.125	1.150	1.175	1.200	1.225	1.250		
0.7	1.018	1.035	1.053	1.071	1.088	1.106	1.124	1.141	1.159	1.176		
0.75	1.014	1.029	1.043	1.057	1.071	1.086	1.100	1.114	1.129	1.143		
0.8	1.011	1.022	1.033	1.044	1.056	1.067	1.078	1.089	1.100	1.111		
0.9	1.005	1.011	1.016	1.021	1.026	1.032	1.037	1.042	1.047	1.053		
Solar source in anticoincidence	R	$CSF = PSF$	0.05	0.1	0.15	0.2	0.25	0.3	0.35	0.4	0.45	0.5
0.1	1.178	1.391	1.651	1.973	2.385	2.929	3.681	4.789	6.586	10.000		
0.2	1.143	1.308	1.500	1.727	2.000	2.333	2.750	3.286	4.000	5.000		
0.25	1.128	1.273	1.439	1.632	1.857	2.125	2.448	2.846	3.348	4.000		
0.3	1.114	1.241	1.385	1.549	1.737	1.955	2.210	2.514	2.881	3.333		
0.4	1.090	1.188	1.295	1.414	1.545	1.692	1.857	2.043	2.256	2.500		
0.5	1.069	1.143	1.222	1.308	1.400	1.500	1.609	1.727	1.857	2.000		
0.6	1.051	1.105	1.162	1.222	1.286	1.353	1.424	1.500	1.581	1.667		
0.7	1.036	1.073	1.112	1.152	1.194	1.237	1.282	1.329	1.378	1.429		
0.75	1.029	1.059	1.090	1.121	1.154	1.188	1.222	1.258	1.295	1.333		
0.8	1.022	1.045	1.069	1.093	1.118	1.143	1.169	1.195	1.222	1.250		
0.9	1.011	1.021	1.032	1.043	1.054	1.065	1.077	1.088	1.099	1.111		

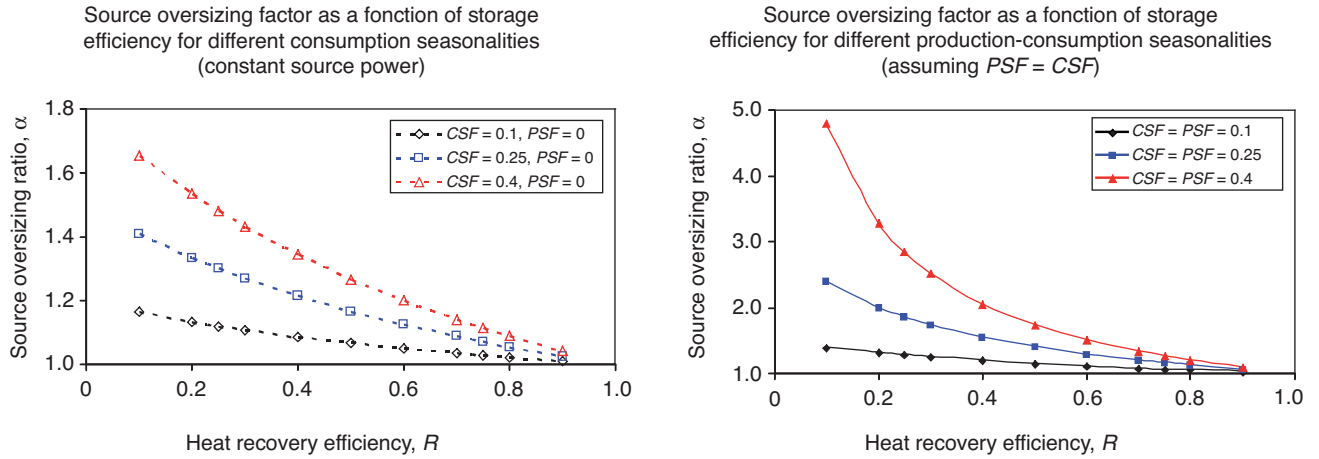


Figure 5

Oversizing ratios as a function of the heat recovery efficiency for various seasonality ratios of the consumption and production (with $\beta = 0.5$).

A bubble shape factor can be defined as the ratio of the hydraulic diameter to the net (*i.e.* porous and permeable) height, that is:

$$\frac{D_h}{H} = \frac{2R_h}{H} = 2\sqrt{\frac{V_{inj}}{\pi\phi H^3}} \quad (10)$$

Considering the above stored volume, an aquifer net height value equal to 25 m and an average porosity of 20%, one determines a hydraulic diameter close to 500 m, corresponding to a hydraulic bubble shape factor equal to 20. That is, the deep aquifer heat stores under consideration herein have a lateral extension of several hundred meters and are fairly flat as long as the net aquifer thickness does not exceed a few tens meters. However, that conclusion has to be moderated in the sense that the thermal bubble size is less than the hydraulic bubble size because of thermal exchanges taking place between the fluid and the solid rock, as discussed in the following.

3.2 Reservoir Heat Losses

Heat losses within the aquifer originates from multiple reasons, including multi-scale conduction phenomena and transport-induced heat dispersion.

Heat dispersion may be caused by:

- a natural hydro-dynamism,
- density and viscosity differences between injected and *in-situ* fluids, leading to thermal segregation and/or fluid flow instabilities,
- but also, very often, by reservoir heterogeneities in terms of permeability.

Obviously, heat dispersion influences the subsequent role played by conduction on temperature or energy distribution

within the reservoir. Reservoir permeability heterogeneity is particularly concerned in this respect.

Actually, *conduction* phenomena occur at different scales:

- at a local scale between the injected fluid and the reservoir constitutive solid medium,
- at the reservoir scale across reservoir bottom and top boundaries: such heat losses result in a non-uniform temperature profile within the store from the wellbore to the thermally-unperturbed surrounding area, as described later on, and,
- at an intermediate scale depending on the reservoir internal structure, between the permeable reservoir zones and embedded impermeable bodies or layers.

3.2.1 Natural Hydrodynamism

If significant, that phenomenon causes a directional migration of the thermal bubble with elapsed time. That phenomenon has to be carefully assessed for small-size low-depth heat storages. As far as deep aquifers are concerned and stored volumes are large, the impact of bubble migration during a storage season remains limited. Indeed, the hydrodynamism of aquifers is reduced with increasing depth, thus resulting in a small migration distance that is still reduced in relative value if bubble size is increased. Considering 1 bar per kilometer (hydraulic height of 10 m per km) as a realistic value of that natural gradient, one infers that the fluid displacement in a 1 Darcy-permeability aquifer is 6 m (for a brine viscosity taken at 0.5 cp), that is in the order of one percent of the hydraulic bubble diameter estimated before. Even considering the smaller diameter of the thermal bubble (as introduced later on), the conclusion of a minor impact of natural hydro-dynamism should remain valid for most deep saline aquifer stores.

3.2.2 Thermal Segregation and Convection

These phenomena may play a role in homogeneous, thick and permeable reservoirs. However, the deep aquifers considered herein have quite often been subjected to a significant diagenesis that tends to emphasize heterogeneities and permeability contrasts within the reservoir. Such heterogeneities actually reduce the effective thickness over which these phenomena can take place. Hence, segregation and convection should be minimal for a good number of deep aquifers, especially carbonate aquifers that are prone to diagenesis and fracturing.

Therefore, we will focus on *conduction* phenomena. In the following, we will assume the initial reservoir temperature is less than the stored fluid temperature.

3.2.3 Local-Scale Conduction: Thermostatic Equilibrium and Thermal Bubble

When hot water is injected in a porous aquifer, an immediate thermal equilibrium establishes between the injected hot water and the rock solid grains, because the characteristic grain size of such porous media lies in the infra-millimetre range. The injected water thermal energy is shared between that injected water and the solid skeleton.

Assuming that local rock-solid thermostatic equilibrium alone and ignoring conduction losses across aquifer limits and heterogeneities, the following energy balance between the injected water heat and the heated porous reservoir volume can then be written at any time of injection:

$$V_{inj} \rho_w c_{pw} (T_{inj} - T_{res}) = \pi \cdot R_{th}^2 \cdot H \cdot [\phi \cdot \rho_w \cdot c_{pw} + (1 - \phi) \cdot \rho_s \cdot c_{ps}] (T_{inj} - T_{res}) \quad (11)$$

with V_{inj} the injected water volume at temperature T_{inj} , T_{res} the initial reservoir temperature, ρ_w and ρ_s the densities of the stored water and of the rock grains, c_{pw} and c_{ps} their respective calorific capacities per mass unit. R_{th} is the “thermal” radius of the heated reservoir area, also denoted as the “thermal bubble” (Fig. 6).

R_{th} is equal to:

$$R_{th} = \sqrt{\frac{V_{inj} \cdot \rho_w \cdot c_{pw}}{\pi \cdot H \cdot [\phi \cdot \rho_w \cdot c_{pw} + (1 - \phi) \cdot \rho_s \cdot c_{ps}]}} \quad (12)$$

Taking into account that $R_h = \sqrt{\frac{V_{inj}}{\phi \cdot \pi \cdot H}}$, one infers that:

$$R_{th} = R_h \cdot \sqrt{\frac{\phi \cdot \rho_w \cdot c_{pw}}{\phi \cdot \rho_w \cdot c_{pw} + (1 - \phi) \cdot \rho_s \cdot c_{ps}}} \quad (13)$$

In the ring $[R_{th}, R_h]$ delimited by the thermal and hydraulic radii, the temperature of the injected fluid equals the initial reservoir temperature because its heat has been taken up by the solid rock in the upstream thermal bubble.

Considering again a porosity of 20% and ($\rho_w, \rho_s, c_{pw}, c_{ps}$) values of (1 g/cm³, 2.7 g/cm³, 4.18 J/(g.°C), 0.84 J/(g.°C)), R_{th} is equal to 0.56 R_h . For the example considered above, R_h and R_{th} are respectively close to 250 and 140 m. For aquifer porosities ranging from 5% to 40%, the thermal radius varies between 30% and 74% of the hydraulic radius. The shape factor of the thermal bubble ranges from one third to three quarters of the swept volume shape factor, which still corresponds to a fairly-flat cylinder for million-plus stored volumes in sedimentary aquifers.

To summarize, considering hot water storage through a vertical well in a fairly-thin aquifer layer, a thermal bubble at temperature T_{inj} gradually extends from the wellbore to the maximal thermal bubble radius, beyond which the fluid-bearing rock remains at the initial reservoir temperature T_{res} .

In reality, because of conduction across reservoir boundaries, a smooth temperature profile actually establishes within the aquifer instead of a steep thermal front, as illustrated in the next sub-section. Therefore, the above estimated value of the thermal bubble radius is only an order of magnitude of the thermally-affected area without any presumption of its thermal quality. In addition, the presence of interspersed impermeable bodies may lead to a flow-controlled dispersion of heat within the reservoir, as also discussed later on in this paper.

3.2.4 Conduction Across Upper and Lower Boundaries

When hot water is injected into a reservoir layer, heat conduction takes place across the bottom and top boundaries of that permeable layer at the same time as the injected hot fluid propagates into the heart of the reservoir (Fig. 6). A non uniform radial profile of temperature results from the superposition of these transport and conduction phenomena. A solution of that problem was derived by Lauwerier (1955) and applied by Butler (1991) for the study of thermal oil recovery processes. Results in radial flow conditions are presented and discussed hereafter for a first storage cycle, which involves the following initial and boundary temperature conditions:

- $T(z,0) = T_{res}$ within the aquifer ($-H/2 < z < +H/2$),
- $T(z,0) = T_{bg} = T_{res}$ in the infinite background ($z < -H/2$ and $z > +H/2$): T_{bg} is varying with depth according to the geothermal gradient, but can be considered as fixed and equal to the initial reservoir temperature T_{res} (herein 60°C) in the immediate environment of a fairly-thin (10-100 m) aquifer,
- Hot water at T_{inj} (herein 90°C) is injected into the aquifer at a constant rate, Q_{inj} , from initial time onwards.

The radial temperature profiles after 180 days of injection of the hot fluid are shown in Figure 7, for different reservoir heights, of 5, 10, 25 and 100 metres. Thermal properties of the reservoir and the neighbouring geological formations are assumed equal.

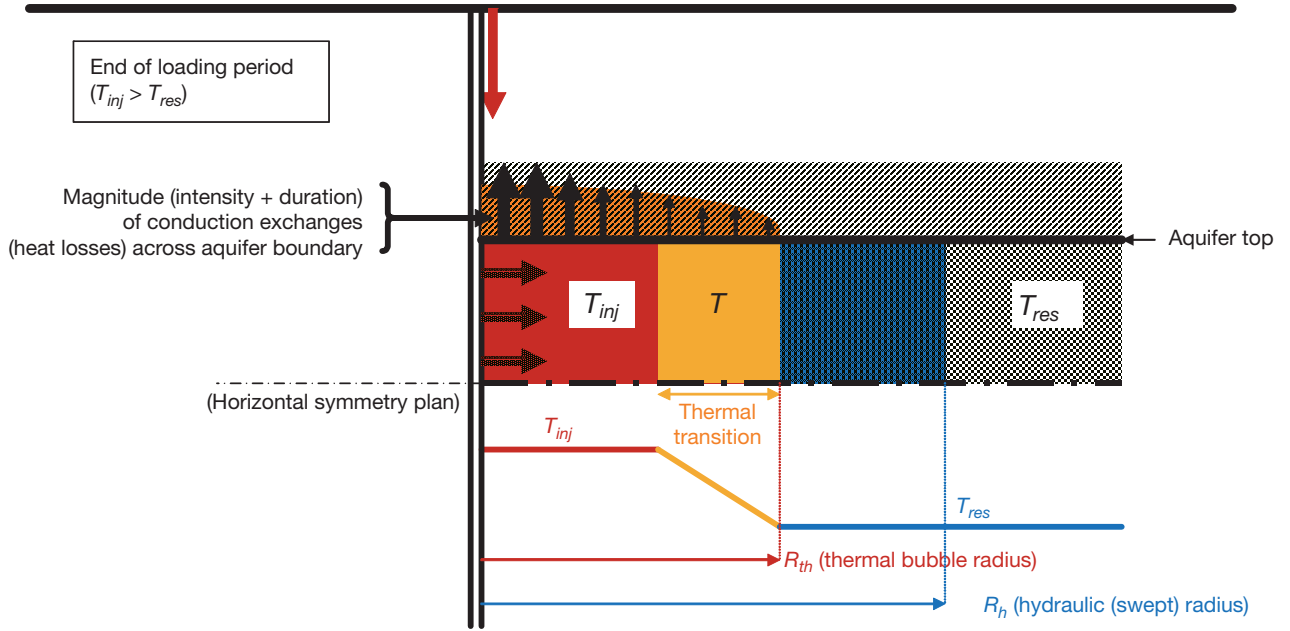


Figure 6

Illustration of thermal exchanges taking place within the aquifer storage – Loading period of the first cycle.

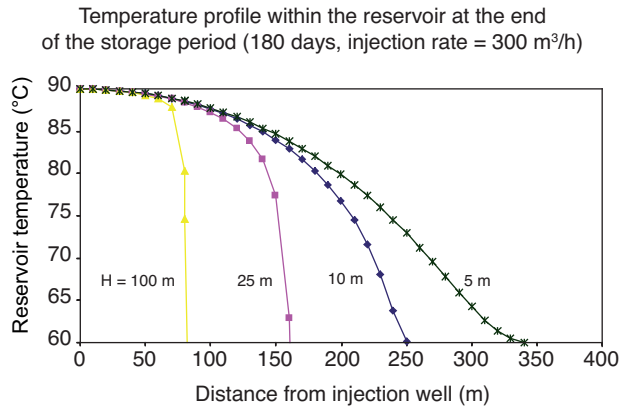


Figure 7

Temperature *versus* distance from wellbore after 180 days of constant-rate injection of a hot fluid ($Q_{inj} = 300 \text{ m}^3/\text{h}$) for different values of the reservoir thickness H . Reservoir temperature $T(r,t)$ is calculated as a function of the elapsed time t and the distance r from injection wellbore, as:

$$T(r,t) = T_{res} + (T_{inj} - T_{res}) \text{erfc}(X), \text{ where:}$$

T_{inj} and T_{res} are the injected fluid temperature (90°C) and initial reservoir temperature (60°C), $X = (x_D/2)[\theta(t_D - x_D)]^{-1/2}$, with:

$$x_D = 4\lambda_{bg}\pi r^2 / (H\rho_w c_{pw} Q_{inj}), \text{ and } \lambda_{bg} \text{ the conductivity of the upper and lower background layers (herein, } 3 \text{ W/(m}\cdot\text{°C))},$$

$$t_D = 4\lambda_{bg}t / (H^2\rho_{sat}c_{psat}) \text{ with } \rho_{sat}c_{psat} = \phi\rho_w c_{pw} + (1 - \phi)\rho_s c_{ps}$$

the heat volumetric capacity of the saturated aquifer rock (herein 2.65 MJ/(m³·°C)),

θ the ratio between the volumetric heat capacity of the aquifer and the one of the upper and lower confining layers (θ is taken equal to 1 herein) and,

erfc the complementary error function.

These temperature profiles can be integrated in order to determine the thermal losses resulting from conduction across reservoir upper/lower boundaries. Results are shown in Table 3. The theoretical thermal front position, R_{th} , that is computed from Equation (12) ignoring any heat losses across aquifer upper/lower boundaries, is also reported. That theoretical front appears to stand a little bit ahead of the very smooth temperature profiles of thin aquifers (Fig. 7) because the stored heat is quasi completely lost by conduction through the surrounding layers after travelling 6 months into such aquifers.

TABLE 3

Reservoir heat losses across upper and lower boundaries at the end of a 6-month storage period at an injection rate of 300 m³/h ((*) values of that column are given for a storage period lasting for only 90 days instead of 180). The radius of the theoretical thermal bubble, R_{th} , is close to the distance from wellbore of the outer edge of Figure 7 temperature profiles

Reservoir thickness (m)	5(*)	5	10	25	100
Heat loss (% of total stored heat)	48.5(*)	57.5	37.3	20.0	7.1
Theoretical thermal radius R_{th} (m)	255(*)	361	255	162	81

Figure 7 and Table 3 indicate that:

- for an aquifer thickness value of 25 m for instance, conduction losses are of 20% of the stored heat after 180 days of injection. Assuming a total restitution of that stored heat during the immediately-starting unloading period, a heat recovery of 80% can be estimated. That assumption of no conduction exchanges during the unloading period is fairly conservative hence acceptable compared to the loading

- period. The reason is that, on its travel back to the wellbore, the pumped hot fluid is set in contact with reservoir limits that are all the hotter as it gets closer to the wellbore;
- for an aquifer thickness decreasing from 100 m to 5 m, conduction losses increase from 7.1% to 57.5% of the stored heat. 10 m may be considered as an order of magnitude of the minimum aquifer thickness below which conduction losses across boundaries become prohibitive, at least for the first storage period. On the opposite, massive aquifers, around 100 m-thick in the example under consideration, constitute optimal reservoirs for heat storage, with conduction heat losses representing less than 10% of the stored energy. One notes that in such aquifers the thermal bubble has a shape factor that is close to unity, *i.e.* 1.6 for the 100 m-thick aquifer case ($D_{th} = 162$ m);
 - for a given aquifer thickness, conduction losses show little sensitivity to the rock porosity because the saturated-rock heat capacity is not very sensitive to the rock porosity. That is, the thermal bubble radius is not much changed by a porosity modification, contrary to the hydraulic radius;
 - a reduction of the storage duration does not efficiently compensate poor reservoir characteristics: for instance, considering a 5 m-thick reservoir, consecutive loading and unloading periods reduced to 3 months each instead of 6 months reduce losses but of much less than half (heat losses decrease from 57.5 to 48.5%, *i.e.* by only 15% in relative value).

The above observations and estimations concern the first storage cycle. At the end of that first injection, the amount of heat lost across boundaries is all the higher as the contact duration with the hot fluid has been longer, *i.e.* all the higher as the distance from injection well is lower. During the subsequent unloading period, a fraction of that lost heat may be recovered by “reverse” conduction, but to a limited extent because the cold fluid pumped from distant reservoir regions contacts heated reservoir boundaries but for time durations that are all the shorter as it gets closer to the wellbore.

The same phenomena are re-iterated during the subsequent loading/unloading cycles but with a lower amplitude than during the first cycle because of decreased temperature gradients across aquifer boundaries. Eventually, the succession of cycles contributes to create and maintain a heated environment for the thermal storage resulting in higher heat recovery efficiencies. Numerical simulations of loading and unloading cycles are required to quantify that temperature distribution. Analytical solutions can only provide an estimate of the thermal evolution of the aquifer taken as a whole.

3.2.5 Conduction-Dispersion Losses as the Result of Internal Aquifer Heterogeneities

The presence of embedded impermeable bodies in the aquifer affects the thermal behaviour of the storage. Depending on the size or thickness of these impermeable bodies or layers, their thermal equilibrium with the flooded reservoir background will be more or less delayed (*Fig. 8*).

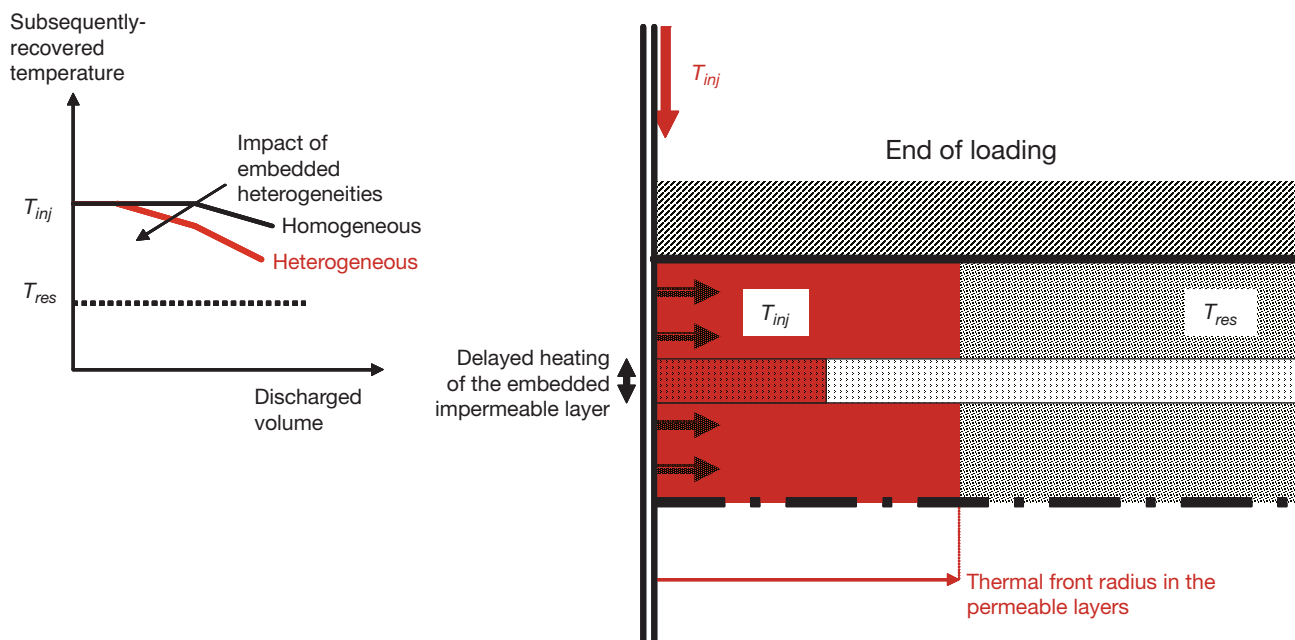


Figure 8

Illustration of thermal exchanges taking place within the aquifer storage in the presence of embedded impermeable layers (loading period of the first cycle).

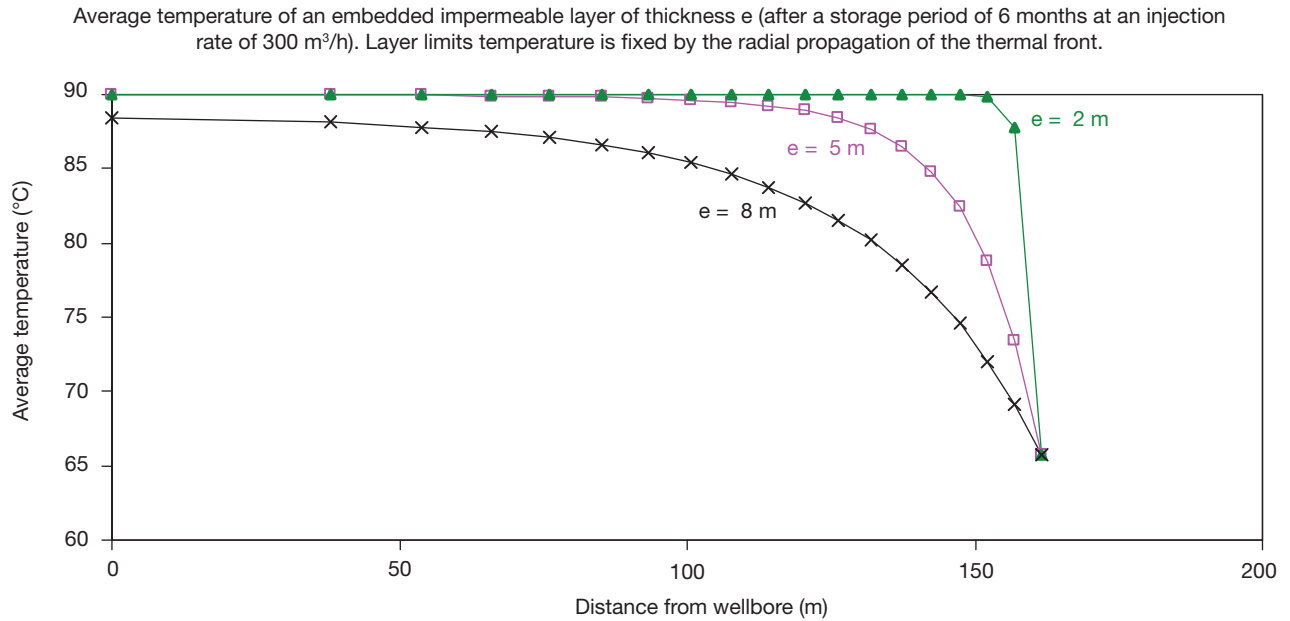


Figure 9

Average temperature profile of an impermeable layer of thickness e embedded in an aquifer at the end of a six-month period of storage of a 90°C fluid injected at a constant rate Q_{inj} of 300 m³/h (the impact of heat losses across the aquifer upper and lower boundaries is ignored and a steep thermal front at 90°C is assumed to propagate into the aquifer: this assumption is valid for layers embedded in the heart of thick aquifers). The average temperature T within the impermeable layer at the distance r from wellbore is then calculated as (Lim and Aziz, 1995):

$$T = T_{res} + (T_{inj} - T_{res}) \{1 - 0.81 \exp[-\pi e \lambda_i (\Delta t_{inj} - t) / (\rho_{sat} c_{psat} e^2)]\}$$
 where:

T_{inj} and T_{res} are the stored fluid temperature (90°C) and the initial reservoir temperature (60°C),

λ_i the conductivity of the impermeable layer (herein, 3 W/(m·°C)),

$\rho_{sat} c_{psat}$ the heat volumetric capacity of the impermeable layer (herein, 2.65 MJ/(m³·°C)),

Δt_{inj} the injection duration (herein, 6 months), t the elapsed time since the beginning of injection when the thermal front is at distance r from wellbore: t and r are related by Equation (12) with $R_m = r$ and $V_{inj} = Q_{inj} t$ (herein, the heat volumetric capacity of the permeable aquifer, *i.e.*

$\phi \rho_w c_{pw} + (1 - \phi) \rho_s c_{ps}$, is assumed equal to that of the impermeable layer, $\rho_{sat} c_{psat}$), and \exp the exponential function.

In order to give an order of magnitude of this phenomenon, we will consider an impermeable layer embedded in the middle of a thick aquifer. We assume the radial propagation of a thermal front of fixed temperature from a wellbore where a hot fluid is injected at a constant flow rate. The impermeable layer boundaries are then subjected to a sudden temperature increment at a time depending on its distance from the wellbore. The resulting evolution of the average temperature within the layer can be estimated by an exponential approximation (Lim and Aziz, 1995) of the solution to that conduction problem (Carslaw and Jaeger, 1959). Results are given in Figure 9 after a storage period of 180 days, with the average temperature of the embedded layer shown as a function of the distance from wellbore, for different layer-thickness values. The main following observations can be made:

- at the end of a storage period of 180 days at 300 m³/h, non-conductive layers more than 2 or several metres in thickness remain below the injection fluid temperature far from wellbore. This means that at the end of the storage period, the area of the thermal bubble will be larger than that of a uniformly-heated homogeneous reservoir of the same overall thickness;

- moreover, after injection is stopped, the rock material of these embedded layers will continue to be reheated by the stored fluid. That is, the stored fluid will be somewhat cooled, leading to lower production temperatures during the subsequent unloading period than in the homogeneous reservoir case;
- however, if the smallest characteristic size of an embedded heterogeneity is low enough, *i.e.* in the order of one meter or less, then it is quasi-instantaneously heated up to the stored fluid temperature so that it behaves as a heat accumulator for the reservoir considered as a whole.

One may then infer the following for the purpose of aquifer selection:

- the presence of small-size impermeable heterogeneities (with a less-than-metric smallest dimension) is not detrimental to the recovery efficiency of the heat storage, since thermal equilibrium with the injected fluid is established over time durations that are negligible compared to the duration of a loading/unloading period. The presence of multiple thin intercalations may even be beneficial because increasing the gross thickness of the aquifer reduces the relative impact of thermal losses across upper and lower aquifer

boundaries while keeping the thermal quality of the recovered heat during the unloading period. Furthermore, the presence of thin low-permeability/tight intercalations within the reservoir annihilates the risk of thermal convection phenomena that exists within thick and permeable aquifers;

- on the contrary, aquifers embedding thick heterogeneities (more than one or several meters in their smallest dimension) are not at thermal equilibrium at the end of the loading period. Hence, their apparent thermal bubble radius is increased but the temperature of the subsequently-recovered fluid starts decreasing sooner and to lower levels than for an equivalent massive reservoir of the same overall thickness.

In summary, small-size impermeable heterogeneities act like a heat accumulator for the aquifer store making it more massive and compact, whereas large/thick heterogeneities reduce the thermal performance of the store.

3.2.6 Conclusion for the Selection and Assessment of an Aquifer

Previous technical discussions on the various origins for thermal losses lead to the following criteria for selecting a deep saline aquifer for heat storage purposes:

- the aquifer should have a sufficient overall thickness to minimize energy losses across its upper and lower boundaries, keeping in mind that such losses show the largest impact during the first storage cycle when the reservoir background has not yet been heated at all by the stored fluid;
- thick (metric or more than metric) impermeable bodies or layers should be absent within the reservoir, in order to preserve a good thermal quality of the unloaded fluid;
- however, the presence of disseminated thin impermeable intercalations may be considered as a favourable criterion as they make thermal bubbles more compact (with a low gross shape factor $\frac{D_m}{H}$) while avoiding the onset of convection phenomena;
- in addition to the above geological features, the aquifer under consideration for heat storage purpose must have a permeability-thickness product that does not restrict the loading/unloading rates to a level below which the impact of transport losses becomes significant, as stated hereafter.

3.3 Transport Losses

Transport losses include all heat losses taking place on each of the two loops linking well bottom-hole and surface exchangers.

In a first approximation, the upstream-downstream temperature drop, $\Delta T = (T_{up} - T_{down})$, of the aqueous fluid circulating at a flow rate q_w in a pipe of curvilinear length L and characterized by a global transfer coefficient A , can be approximated as:

$$\Delta T = T_{up} - T_{down} = (T_{up} - T_{env}) \frac{AL}{\rho_w \cdot c_{pw} \cdot q_w} \quad (14)$$

where T_{up} and T_{down} are respectively the upstream and the downstream fluid temperatures, and T_{env} is the temperature of the environment (atmosphere or soil) surrounding the pipe.

Fluid travel lengths are the elementary aerial or/and buried distances linking the heat network or the heat source and the bottom-hole of aquifer storage wells. The location and depth of favourable aquifer sites with respect to the heat production and consumption points then determines the values of these lengths.

Further pipe insulation may minimize the global transfer coefficient, A .

Therefore, for given thermal conditions of the source, the reservoir, the heat network and the fluid travel environments, the only remaining variable is the injection/production flow rate. Provided that installations, including conduits and exchangers, are properly sized, increasing the storage flow rate minimizes thermal transport losses. That is, as far as single and massive source and consumption points are concerned, the highest thermal recovery efficiency is obtained for maximum flow rates via a minimized number of wells. That situation also minimizes the capital expenditure.

However, the deliverability of the reservoir is often a limiting factor for the well flow rate. At that point, the question of choice of an optimal well geometry may be raised. A deviated trajectory improves the productivity/injectivity to a limited extent, depending on the deviation angle and the vertical-to-horizontal permeability anisotropy. A horizontal trajectory may be considered, but only for fairly massive and vertically-homogeneous reservoirs; that option may then appear as risky if aquifer heterogeneities have not been carefully characterized.

Therefore, taking into account these geological risks as well as drilling overcosts, a deviated well trajectory appears as the best compromise, inasmuch as that option maximizes the interception of various aquifer conductive layers. For fairly-deep (more than 1 km) aquifers, deviated wells may also reach independent heat bubbles from nearby wellheads.

Maintaining the productivity/injectivity of wells over many annual storage cycles probably constitutes the main challenge of an Aquifer Thermal Energy Storage project. Indeed, temperature changes undergone by the aquifer during loading and unloading periods may alter the rock-fluid geochemical equilibrium and induce precipitation/dissolution phenomena. Moreover, temperature changes in combination with fluid-property change or contaminants (oxygen, corrosion products released by conduits, well tubing and casing, etc.) may favour a biologic activity that may enhance corrosion phenomena. Therefore, the possible occurrence of such phenomena has to be carefully considered before

implementing an ATEs. The risks of equipment degradation and reservoir performance loss with time may then be minimized through the choice of proper materials and through the design of a permanent surveillance programme, including preventive operations or maintenance.

Actually, a significant drop of well performance turns out very rapidly into a non-economic situation for the heat store project. An increased pressure drop firstly increases the electricity consumption of the pumps, then beyond a certain limit, pumping rates can no more be sustained and heat losses start increasing. That is, well performance decline results in both a lower amount and a lower thermal quality of the recovered heat.

CONCLUSION: DEEP SALINE AQUIFER SELECTION CRITERIA FOR HEAT STORAGE PURPOSES

Deep saline aquifers are not subjected to so-restrictive usage conditions as low-depth fresh/potable water aquifers are. Any kind of exploitation may even be prohibited for strategic aquifers considered as future or spare potable water resources. Therefore, deep saline aquifers may appear as the preferred option for implementing an ATEs project.

However, the economic viability of such a project has to be proved, which goes through a careful assessment of the heat recovery efficiency of the aquifer storage and of project costs.

First of all, the need to resort to an ATEs solution to optimize energy use has to be appreciated from a quantification of the present and future misfit between available heat sources and consumption. That seasonal misfit determines the project size in terms of brine stored volume and transfer rate to or from the aquifer storage.

The qualification of an aquifer as a possible candidate for storage must then be undertaken on the basis of the estimation of its thermal recovery performance. The overall parameter review presented herein revealed the necessity of collecting and integrating any available data characterizing the geometry and internal (heterogeneous) structure of the aquifer as well as its dynamic behaviour. All geological and petrophysical parameters leading to a compact-shape thermal bubble were shown to maximize the performance of the storage in terms of recovered energy and temperature, including a large thickness and the presence of small-scale heterogeneities acting as “fast-response heat accumulators”. A very high deliverability is also a determinant factor of energetic performance as high well rates minimize heat losses in conduits. Numerical simulations of storage cycles are recommended to perform sensitivity studies to uncertain aquifer characteristics, and to determine the possible range of aquifer recovery performance values and their evolution with cycling.

Finally, storage benefits in terms of saved/valorised heat have to be confronted to involved costs, among which capital expenditure linked to wells represents a major contribution. That confrontation, *i.e.* economic viability assessment, determines the final decision of implementing the ATEs project.

Considering that well costs increase more than linearly with depth whereas heat losses tend to decrease linearly with depth (due to a roughly-constant geothermal gradient), a general aquifer selection criterion for ATEs application would lie in a depth compromise that minimizes capital expenditure below the strategic fresh-water aquifers limit while satisfying optimal reservoir characteristics that maximize the heat recovery performance.

REFERENCES

- ADEME brochure: “Maîtrise de l’énergie et énergies renouvelables - Chiffres clés 2007”, can be downloaded from website: <http://www2.ademe.fr/servlet/getDoc?cid=96&m=3&id=58309&p1=00&p2=07&ref=17597>.
- Busso A., Georgiev A., Roth P. (2003) Underground Thermal Energy Storage – First Thermal Response Test in South America, *Proceedings World Climate & Energy Event*, Rio de Janeiro, Brazil, 1-5 December 2003.
- Butler R.M. (1991) Convective Heating within Reservoirs, in *Thermal Recovery of Oil & Bitumen*, Prentice-Hall, Englewood Cliffs.
- Carslaw H.S., Jaeger J.C. (1959) *Conduction of heat in solids*, 2nd ed., Clarendon Press, Oxford.
- Cormary Y., Iris P., Marie J.P., de Marsily G., Michel H., Zaquine M.F. (1978) Heat Storage in a Phreatic Aquifer: Campuget Experiment (Gard, France), *Proceedings of Thermal Energy Storage in Aquifers workshop*, pp. 88-93.
- Dickinson J.S., Buik N., Matthews M.C., Snijders A. (2009) Aquifer Thermal Energy Storage: Theoretical and Operational Analysis, *Géotechnique* **59**, 3, 249-260.
- Housse B.A., Despois J. (1985) Prototype of an Underground Heat Storage System at Thiverval-Grignon (France), *Proceedings of Enerstock 85 – 3rd International Conference on Energy Storage for Building Heating and Cooling*, Sept. 22-26, pp. 71-74.
- Kabus F., Hoffmann F., Möllmann G. (2005) Aquifer Storage of Waste Heat Arising from a Gas and Steam Cogeneration Plant – Concept and First Operating Experience, *Proceedings World Geothermal Congress 2005*, Antalya, Turkey, 24-29 April.
- Kazmann R.G. (1978) Underground hot water storage could cut national fuel needs 10%. *Civil Engineering – Am. Soc. of Civil Eng.*, 57-60, May 1978.
- Lau K.C., Mirza C., Crawford A.M., Morofsky E.L. (1986) Initial Experiences with the Canada Centre ATEs, *Proceedings of the Intersociety Energy Conversion Engineering Conference*, published by the American Chemical Society, pp. 676-681.
- Lauwerier H.A. (1955) The Transport of Heat in an Oil Layer Caused by the Injection of Hot Fluid, *Appl. Sci. Res.* **5**, 145-150.
- Letz T. (2004) Suivi des Systèmes Solaires Combinés: Guide méthodologique (mise à jour 2004), document web address: <http://www.ines-solaire.com/pdf/guide%20suivis%20SSC%202004.pdf>.
- Lim K.T., Aziz K. (1995) Matrix-Fracture Transfer Shape Factors for Dual-Porosity Simulators, *J. Petrol. Sci. Eng.* **13**, 169-178.

- Miller R.T. (1986) Thermal-Energy Storage in a Deep Sandstone Aquifer in Minnesota: Field Observations and Thermal Energy-Transport Modeling, *Proceedings of the Intersociety Energy Conversion Engineering Conference*, published by the American Chemical Society, pp. 682-685.
- Molz F.J., Warman J.C. (Auburn U., Alabama) (1978) Confined Aquifer Experiment – Heat Storage. Thermal Energy Storage in Aquifers Workshop.
- Molz F.J., Raymond J.R. (1984) Store Heat Underground. Or What to do When the Sun Goes Down, *Chemtech.*, December 1984, 752-755.
- Sanner B., Kabus F., Seibt P., Bartels J. (2005) Underground Thermal Energy Storage for the German Parliament in Berlin, System Concept and Operational Experiences, *Proceedings World Geothermal Congress 2005*, Antalya, Turkey, 24-29 April.
- Saugy B. (1990) SPEOS sept ans après. *Gaz-Eaux-Eaux Usées* **70**, 6, 397-406.
- Schmidt T., Mangold D., Müller-Steinhagen H. (2003) Seasonal Thermal Energy Storage in German, *ISES Solar World Congress 2003*, Göteborg, Sweden, 14-19 June.
- Ungerer P., Le Bel L. (2006) Le stockage de chaleur en aquifère : une nouvelle perspective pour la géothermie, Dossier : Stockage de l'Énergie, *Revue des Ingénieurs des Mines* **423**, Nov./Déc. 2006, 35-37.

*Final manuscript received in July 2010
Published online in February 2011*

Copyright © 2011 IFP Energies nouvelles

Permission to make digital or hard copies of part or all of this work for personal or classroom use is granted without fee provided that copies are not made or distributed for profit or commercial advantage and that copies bear this notice and the full citation on the first page. Copyrights for components of this work owned by others than IFP Energies nouvelles must be honored. Abstracting with credit is permitted. To copy otherwise, to republish, to post on servers, or to redistribute to lists, requires prior specific permission and/or a fee: Request permission from Information Mission, IFP Energies nouvelles, fax. +33 1 47 52 70 96, or revueogst@ifpen.fr.